Frequency and damping ratio assessment of high-rise buildings using an Automatic Model-Based Approach applied to real-world ambient vibration recordings

Fatima Nasser, Zhongyang Li, Philippe Gueguen, Nadine Martin

Frequency and Damping Ratio Assessment of High-Rise Buildings using an Automatic Model-Based Approach applied to Real-World Ambient Vibration Recordings

Fatima Nasser[a,*], Zhongyang Li[a], Philippe Gueguen[b], Nadine Martin[a]

[a] *Gipsa-lab, Departement Images Signal*
BP 46-961 F-38402 Saint Martin d'Heres, France
[b] *ISTerre, Univ. Grenoble /CNRS/IFSTTAR*
BP 53, 38041 Grenoble cedex 9, France

Abstract

This paper deals with the application of the Automatic Model-Based Approach (AMBA) over actual buildings subjected to real-world ambient vibrations. In a previous paper AMBA was developed with the aim of automating the estimation process of the modal parameters and minimizing the estimation error, especially that of the damping ratio. It is applicable over a single-channel record, has no parameters to be set, and no manual initialization phase. The results present in this paper should be regarded as further documentation of the approach over real-world ambient vibration signals.

Keywords: Automatic modal parameter estimation, real-world ambient vibrations, Multi-mode Random Decrement Signature, Filter-free Random Decrement Technique, high-rise actual buildings.

---

1. Introduction

This paper is the continuing part of a study that deals with an automatic modal estimate of multi-component signals of high-rise buildings subjected to

*Corresponding author
Email addresses: `fatima.nasser@gipsa-lab.grenoble-inp.fr` (Fatima Nasser), `zhong-yang.li@gipsa-lab.grenoble-inp.fr` (Zhongyang Li), `Pilippe.gueguen@obs.ujf-grenoble.fr` (Philippe Gueguen), `nadine.martin@gipsa-lab.grenoble-inp.fr` (Nadine Martin)

ambient vibrations. In the first part of this study [1], an Automatic Model-Based Approach (AMBA) was proposed and demonstrated on simulated signals. This paper aims to demonstrate its performance on real-world applications.

AMBA works with what we called a Multi-mode Random Decrement Signature (MRDS). The MRDS is estimated via omitting the filtering process prior to the application of the Random Decrement Technique (RDT). As to define the number of modes of the estimated MRDS, the approach starts by a spectral-based initialization step. This step serves two main benefits, first, it defines the number of modes in the MRDS under study via an automatic peak detection method. Second, it gives a rough and biased estimation of both the frequency and the damping ratio of each of the defined modes. The proposed approach ends up with a final non-biased modal estimation using the maximum likelihood procedure. These steps make the proposed approach AMBA of [1] applicable over a single-channel record of multi-mode signals despite of the noise level. The mathematics of AMBA, along with its theoretical concept are presented in full details in the previous part of this study [1].

In [1] an extensive validation of AMBA has been carried out over simulated data which were generated from a model of high-rise building defined as a continuous beam [2, 3]. The results have proven that AMBA is reliable, efficient and robust in estimating the natural frequencies and damping ratios of signals of different types, *e.g.* well-spaced modes, quasi-spaced modes, and closely-spaced modes. However, one of the perspectives of [1] was to further validate the proposed approach over real-world ambient vibration recordings. This paper responds to such a need.

To this end, the current paper presents the validation of AMBA method over six actual buildings subjected to real-world ambient vibrations. Three of these buildings are located in Beirut (Lebanon), and three others are located in Grenoble (France). These buildings are chosen due to their interesting characteristics and to the extensive analysis that was performed to estimate their modal parameters [4, 5, 6, 7, 8, 9]. Such prior analysis of these buildings provides a good database for comparisons and allows to validate AMBA.

The remainder of this paper is organized as follows: section 2 briefly presents the physical and the signal models used in [1] to deal with AMBA. Then the necessary overview of the general aspect of AMBA is given in section 3. Section 4 presents the methodology proposed in this paper to automatically choose the best length of the MRDS in terms of number of fundamental periods, referred to as an N_{rds} in AMBA. Section 5 presents the description of the six chosen buildings (structure, design, height, materials, *etc.*), along with the already estimated modal values of these buildings in the literature. The analysis and discussion of the obtained results of the six buildings by AMBA are detailed in section 6. Finally, section 7 draws the conclusions.

2. Physical and Signal Model

In order to understand each step of AMBA, a brief introduction of the physical and the proposed signal models in [1] are first presented in this section.

Physically, the measured building vibration $y[n]$ is given as

$$\begin{aligned} y[n] &= \mathfrak{g}[\mathfrak{n}] + e[n], \\ \text{where} \quad \mathfrak{g}[\mathfrak{n}] &= h[n] * p[n] \end{aligned} \tag{1}$$

$$\text{with} \quad h[n] = \sum_{k=1}^{K} A_{0k} \exp^{-2\pi f_k \xi_k n} \sin(\omega_{Dk} n + \varphi_{0k}), \forall k \in [1, K], \tag{2}$$

where n is the discrete time index, $\mathfrak{g}[\mathfrak{n}]$ is the noise-free part of the building vibration, $h[n]$ is the impulse response of a building. The initial amplitude ($A_{0k} = -1/\omega_{Dk}$) , the damping ratio (ξ_k), the natural frequency (f_k), the initial phase (φ_{0k}), and the number of modes (K) are the parameters that feature $h[n]$. $\omega_{Dk} = 2\pi f_k \sqrt{1-\xi_k^2}$ is the damped pseudo-pulsation, $p[n]$ and $e[n]$ are the seismic and the additive noises respectively, both assumed to be white Gaussian of zero mean and unknown variance. $*$ is the convolution operator. It is worth mentioning that we consider the seismic noise as the overall impact of the seismic base motion and some other noise sources, such as the wind, waterflow, traffic *etc.* In this paper, the overall seismic noise is considered as a stationary Gaussian random excitation.

The Random Decrement Technique (RDT) is a method capable of extracting the building vibration signal and providing a free-decay signature equivalent to the system impulse response. The concept of the RDT [10] simply states that at any given time, the ambient vibrations are the forced responses of the building excited by the seismic noise. By stacking and averaging a sufficient number of segments whose initial conditions are the same, the forced vibration response component is reduced to zero, then an impulse estimation is revealed in the form of a Random Decrement Signature (RDS).

An RDS is characterized by the same damping ratio ξ_k, natural frequency f_k, and number of modes K as the impulse response $h[n]$ (Eq. (2)), but not the initial phase, and the initial amplitude, as these two parameters are changed due to the averaging principle of the RDT.

As per [1], the main interest of using AMBA is to estimate simultaneously and automatically all the frequencies and the damping ratios of the signal from a Multi-mode RDS referred to as an MRDS.

Considering all the above, in [1] the model of an MRDS $s[n]$ is assumed as

$$s[n] = \mathfrak{h}[\mathfrak{n}] + v[n], \tag{3}$$

$$\text{with} \quad \mathfrak{h}[\mathfrak{n}] = \sum_{k=1}^{K} B_{0k} \text{exp}^{-2\pi f_k \xi_k n} \sin(2\pi f_k n + \varphi_{0k}), \forall k \in [1, K], \tag{4}$$

where $v[n]$ is the residue of the RDT considered as an additive white Gaussian noise with zero mean and unknown variance. $\mathfrak{h}[\mathfrak{n}]$ is a deterministic multi-mode process that keeps the same characteristics as $h[n]$ of Eq. (2) but not for the initial amplitude B_{0k} and the initial phase φ_{0k}. It should be noted that the term $\sqrt{1-\xi_k^2}$ of Eq. (2) is approximately equal to 1 in the considered signal model due to the fact that the range of the damping ratio in the real-world cases is rarely greater than 10%.

3. Overview of AMBA

The Automatic Model Based Approach (AMBA) proposed in [1] is illustrated in Fig. 1 and briefly summarized in three steps as follows:

1. A Filter-Free Random Decrement Technique is applied over $y[n]$ yielding an MRDS $s[n]$ at the output which in turn is decimated before being processed by the second step to reduce the computation time.
2. An initialization step serves mainly to provide a first estimation of the parameters of the noise-free part $\mathfrak{h}[\mathfrak{n}]$ from the MRDS such as the number of modes $\hat{K}$, the frequencies $\hat{f}'_k$, and the damping ratios $\hat{\xi}'_k$.
3. A Maximum-Likelihood Estimator for a refinement parameter estimation of $\mathfrak{h}[\mathfrak{n}]$. As this leads to a multivariate nonlinear function to be optimized, the simulated annealing is used [11].

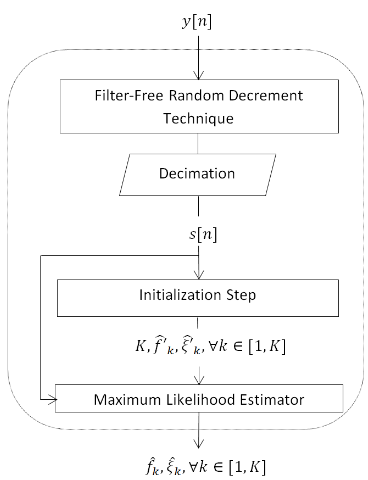

Figure 1: Global flowchart of the Automatic Model-Based Approach (AMBA).

4. Application of AMBA over actual Buildings subjected To Real-World Ambient Vibrations

When performing modal analysis over real-world ambient vibration recordings of actual buildings, we have no *a priori* information of how many modes are in the signal under study, neither on the values of their frequencies nor their damping ratios. To this end, AMBA is initialized by a step that defines roughly the number of modes in the signal under study, thanks to an automatic peak-detection method [1], along with their frequencies and damping ratios. However, this step is spectral-based, *i.e.*, the definition of the number of modes is totally dependent on the frequency resolution of the Welch spectrum.

As the frequency resolution of the Welch spectrum increases with the length of the MRDS (N_{rds}), we decided in this paper to apply AMBA over the whole range of N_{rds} that was precised in [1], that is to say, in the range of 3 to 12 periods.

To select the best N_{rds}, we propose to calculate a normalized error E between $s[n]$ and the reconstructed one $\hat{s}[n]$ based on the estimated parameters

$$E = \frac{\sum_n |s[n] - \hat{s}[n]|^2}{\sum_n (s[n])^2}. \tag{5}$$

Consider all the above, the best N_{rds} that is able to give the most reliable and robust estimation among the others is the one that is able to:

- detect the maximum number of modes as long as a physical interpretation can be established,
- provide the most stable damping ratio estimation, along with the most stable normalized error, E (Eq. 5), with respect to N_{rds}.

These criteria are applied throughout the whole validation process of AMBA over all the chosen actual buildings in this article.

5. Description of the Six Buildings under Study

In this study, we validate AMBA over six actual high-rise buildings subjected to real-world ambient vibrations, three of them are in Beirut (Lebanon) and the other three are in Grenoble (France). These buildings are selected because of their interesting characteristics, they are all regular in plan and in elevation, they are all constructed in reinforced concrete with shear walls, and the velocimeter was always placed at the top of the building in the middle of the last floor.

The buildings of Beirut (Fig. 2 (a)) are the three towers of the Cap-sur-ville project. They were constructed in 1995 in the Eastern side of Beirut. Following [4], the tower with 21 stories is named W, the other two towers with 18 and 16 stories are named V and X respectively.

Based on [4], the construction design is the same for the three towers, they are all designed in reinforced concrete panels fixed to reinforced concrete frame elements, and settled inside the sandstone at 20 m depth. These towers are about 50 m apart from each other, and they are all constructed over the same geological formations. Two stories of car park occupy most of the buried foundation part of the three towers. The only difference is in terms of height, as each of them has different number of stories.

In [4] they detailed that each tower is instrumented at the top with a Taurus seismic station (Nanometrics) associated to a velocimeter. This sensor has a frequency response in the 0.033 - 40 Hz frequency band. The sampling frequency is 200 Hz

The three buildings of Grenoble (France) are Mont-Blanc, Belledonne, and Arpej II towers. Mont-Blanc and Belledonne are two of the three Ile Verte towers (Fig. 2 (b)). In [5, 6] they studied these buildings and provided a full description of their structure as follows; these stand-alone towers are 30-story reinforced concrete buildings. The structure is a rhombus of 40×20 m. The velocimeter is used at the top of each building to record the ambient vibrations. The sampling frequency is set to 50 Hz.

Following [6, 7], Arpej II is one of the two twin 16-storey reinforced concrete buildings (Length $\times$ Thickness $\times$ Height $= 28 \times 12 \times 56$ m) built in the 1970s on the Grenoble university campus (Fig. 2 (c)). The storey height is regular between the 2^{nd} and 16^{th} floors (3.3 m) and taller at the first floor (5.5 m). Its structure is composed of a reinforced concrete frame with two reinforced concrete shear walls at the extremities in the transverse direction and an reinforced concrete shear wall core for lift shafts and stairwells. The ambient vibrations of Arpej II were recorded at the top of the building using a velocimeter. The sampling frequency is set to 200 Hz.

(a) (b) (c)

Figure 2: Perspective view of (a) the three towers W, V and X of the Cap-sur-ville project in Beirut (Lebanon). (b) Belledonne and Mont-Blanc towers, and (c) Arpej II tower in Grenoble (France).

The real-world ambient vibration recordings of the signals considered in this paper are of different durations. Tab. 1 presents the length of each of the signals. These lengths are converted into number of periods using the following formula

$$N_{sig} = \frac{L_{sig} \times min(\tilde{f})}{F_s}, \tag{6}$$

where N_{sig} is the number of periods of the minimal frequency within the total length of the signal, L_{sig} is the length of the signal in points, $min(\tilde{f})$ being the minimum frequency detected over the signal under study by the automatic peak-detection method (the reader interested by the details of this method can refer to [1]), and F_s is the sampling frequency (Hz).

AMBA is applied over all the considered signals of this paper in the longitudinal direction. The estimated MRDS, from the first step of AMBA, is then decimated to a Nyquist rate of 20 Hz to reduce computation time. This decimation value is equal for all the signals of towers W, X, V, and Arpej II as they have the same sampling frequency of 200 Hz. The signals of Mont-Blanc and Belledonne are not decimated as their sampling frequency is already small (50 Hz).

The results of [4, 5, 6, 7] presented in tables 2 and 3 are used as a reference for comparing with the obtained results by AMBA in this paper.

Signal length	W	V	X	Mont-Blanc	Belledonne	Arpej II
L_{sig} (Points)	720000	720000	720000	174000	174000	180000
L (minutes)	60	60	60	58	58	15
N_{sig} (Periods)	2592	3348	3024	2958	3062	1143

Table 1: The length of the six studied signals measured at Beirut (W, V and X) and at Grenoble (Mont-Blanc, Belledonne and Arpej II).

mode	Tower W Long. (Hz)	Tower V Long. (Hz)	Tower X Long. (Hz)
1	0.72	0.84	0.93
2	*1.16*	*1.34*	*1.46*
3	2.39	2.83	3.15
4	*3.51*	*4.10*	*4.52*
5	4.57	5.30	5.92
6	*6.41*	*7.26*	*8.12*
7	6.92	NA	NA

Table 2: The modal frequency values of towers W, V, and X estimated in [4] using Fast Fourier Transform applied over ambient vibration recordings made in the three towers in the longitudinal (Long.) direction. Italic values are related to the torsion modes that are observed in Long. direction. (This table is modified after [4]).

Velocimeter					
	Freq. (Hz)- Long.		Freq. (Hz)-Trans.		Freq. (Hz) Torsion
	Mode 1	Mode 2	Mode 1	Mode 2	
Arpej II	1.27	4.96	1.12	4.37	1.37
Mont-Blanc	0.85	3.26	0.66	2.64	0.96
Belledonne	0.88	3.17	0.68	2.78	1.00

Table 3: The modal frequency values of towers Arpej II, Mont-Blanc and Belledonne estimated by [7] using Fourier analysis and Frequency Domain Decomposition of ambient vibrations. Long. and Trans. indicates the estimation in Longitudinal and Transverse directions respectively.

Starting with the three towers of Beirut, the authors of [4] found that the same fundamental frequency is obtained in the two horizontal directions for the three towers. Considering the towers as continuous beams, they observed the classical series of bending frequencies (fundamental and overtones) for shear beam in the three towers (*i.e.*, $f_2/f_1 = 3, f_3/f_1 = 5, f_4/f_1 = 7$) in the longitudinal direction. As a consequence, they assumed the intermediate frequencies, the ones in italic case in Tab. 2, to be corresponding to the torsion mode that is only observed on the longitudinal direction for towers W and V, and on both horizontal components for tower X. According to [4] such observations are considered as the proof of some variations of the building design of the tower X. As per [4], Fig. 3 (a) presents the spectral analysis of the signals of the three towers W, V and X.

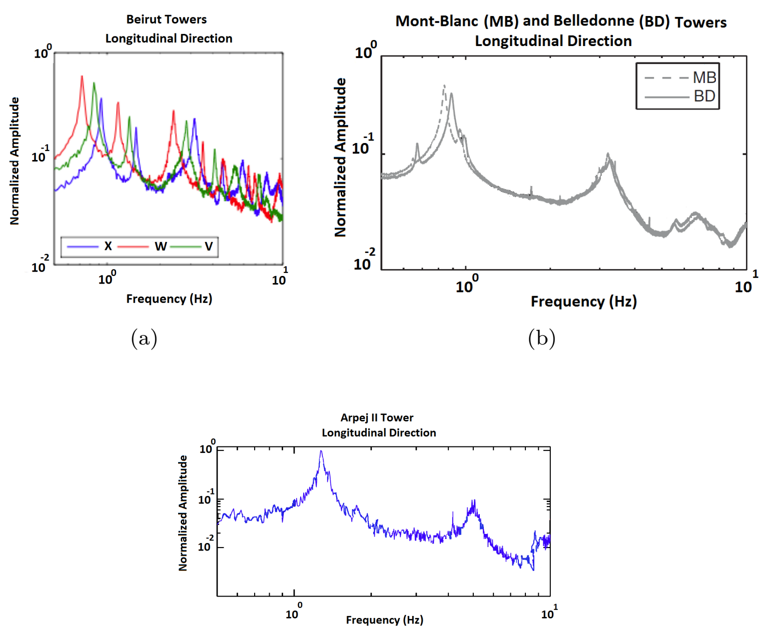

(a) (b)

(c)

Figure 3: The FFT computed using the ambinet vibrations recorded at the top of (a) the three towers W, V and X of the Cap-sur-ville project in Beirut (Lebanon) [4], (b) Belledonne and Mont-Blanc towers, and (c) Arpej II tower in Grenoble (France) [7].

As per [5], the behavior of Mont-Blanc and Belledonne is quite similar. Their fundamental modes are found at 0.65 Hz (Transverse) and 0.84 Hz (Longitudinal) and 0.67 Hz (Transverse) and 0.89 Hz (Longitudinal) for Mont-Blanc and Belledonne towers respectively. The longitudinal modes are clearly presented in the spectral analysis of Fig. 3 (b). A torsion mode was observed close to 1

Hz. All these values were also observed by [6] using an extensive modal analysis with multichannel recordings.

In [5, 6], they illustrated that even though Mont-Blanc and Belledonne towers can be considered as being perfectly identical in terms of design, shape and height, the obtained modal frequency values provide information on the existence of slight differences due to the presence of differences in design or due to the elastic property variations.

Following [7], the first two modes of Arpej II tower at 1.27 Hz and 4.96 Hz were detected on the Fourier spectrum as shown in Fig. 3 (c) in the longitudinal direction. A torsion mode was also found at around 1.37 Hz.

6. AMBA method: Result analysis and discussion

The estimated frequency and damping ratio values that are assessed by AMBA when applied on towers W, X and V in Beirut are respectively presented in figures (4, 6, and 7), and on towers Mont-Blanc, Belledonne, and Arpej II in Grenoble are as well respectively illustrated in figures (8, 9, and 10). Each of the aforementioned figures contain three subfigures: (a) the estimated frequency Hz, (b) the estimated damping ratio %, and (c) the normalized error, E (Eq. 5). The abscissa for all the figures are the number of periods of the MRDS (N_{rds}) varying from 3 to 12 periods. For the sake of clarity, different scales were used for different figures. The different modes are associated by the same color and the same line style between subfigures (a) and (b) in all the figures.

All of these figures are split into different regions by a vertical black line, based on the values of the N_{rds} and the associated estimates of frequency and damping ratio. The splitting process is mainly related to the criteria of automatically classifying the best N_{rds} that is able to carry out the most reliable estimates, as discussed earlier in section 4, *i.e.*, the best N_{rds} is the one that is able to detect the maximum number of modes, and provide the most stable damping ratio estimation, along with the most stable normalized error, E.

First, the region with the highest number of detected modes is identified, then the following steps are applied uniquely over this region:

1. The normalized error E as in Eq. 5 is calculated;
2. The standard deviation σ_E of these errors is also computed using

$$S = \frac{1}{C-1} \sum_{i=1}^{C} |\hat{x}_i - \bar{x}|^2, \tag{7}$$

   where C is the number of the noise realizations, $\hat{x}_i$ is the estimated value of the frequency or the damping ratio $\forall i \in [1, C]$, and $\bar{x_i}$ is the mean value of the estiamted values of the frequency or the damping ratio with $\bar{x} = \frac{1}{C} \sum_{i=1}^{C} \hat{x}_i$.
3. The smallest σ_E is highlighted for the region of interest among the other regions,
4. Finally, the mean estimate of the associated frequency and damping ratio of the regions of interest are calculated. These values are presented in Tabs. 4 and 5 for the buildings of Beirut and Grenoble respectively.

In order to validate the correctness of the obtained results, we compared the mean values of the estimated frequencies to the work of [4, 5, 6, 7]. The comparison for the towers of Beirut and Grenoble is presented in Figs. (5 and 11) respectively.

It is worth mentioning that for [4, 5, 6, 7], the analysis was more focused on frequency estimation rather than damping estimation. Only the damping values of the fundamental modes of Grenoble towers were estimated by them. These values were estimated using the RDT accompained with the logarithmic decrement classical method as 0.58 %, 1.09 % and 1.12 % for Mont-Blanc, Belledonne and Arpej II towers respectively. The estiamted damping values show a very well accordance with the values extracted by AMBA and presented in Tab. 5. They show an almost trivial normalized error e of 2.73 %, 5.50 % and 5.35 % for Mont-Blanc, Belledonne and Arpej II respectively, with $e = \frac{\xi - \xi_i}{\xi} \times 100$ where ξ is the damping value estimated by the logarithmic decrement method, and ξ_i is the one estimated by AMBA.

	Tower W						Tower V						Tower X					
Region of interest	$8 \le N_{rds} \le 10$						$6 \le N_{rds} \le 8$						$10 \le N_{rds} \le 12$					
mode	$\bar{f}$	σ_f	$\hat{C}_f$	$\bar{\xi}$	σ_ξ	$\hat{C}_\xi$	$\bar{f}$	σ_f	$\hat{C}_f$	$\bar{\xi}$	σ_ξ	$\hat{C}_\xi$	$\bar{f}$	σ_f	$\hat{C}_f$	$\bar{\xi}$	σ_ξ	$\hat{C}_\xi$
1	0.69	0.0010	0.1449	0.68	0.0173	2.5441	0.83	0.0057	0.6867	0.80	0.0306	3.825	0.90	0.0035	0.3888	0.59	0.0057	0.9661
2	*1.13*	0.0065	0.5752	0.80	0.0577	7.2125	*1.30*	0.0058	0.4461	0.60	0.1442	24.033	*1.43*	0.0061	0.4265	0.59	0.0119	2.0169
3	2.37	0.0057	0.2405	0.97	0.0100	1.0309	2.81	0.00058	0.0206	1.27	0.0306	2.4094	3.12	0.0058	0.1858	1.15	0.0503	4.3739
4	*3.48*	0.0058	0.1666	0.57	0.0173	3.0350	*4.06*	0.0058	0.1428	0.69	0.0635	9.2028	*4.50*	0.0058	0.1288	0.91	0.0228	2.5054
5	4.52	0.0017	0.0376	1.86	0.0173	0.9301	5.57	0.0417	0.7486	1.16	0.0200	1.7241	5.92	0.0172	0.2905	0.84	0.0300	3.5714
6	*6.46*	0.011	0.1702	0.55	0.0451	8.2000	*7.49*	0.0936	1.2496	1.07	0.1002	9.3644	*8.07*	0.0172	0.2131	0.33	0.0308	9.3333
7	6.88	0.011	0.1598	1.68	0.0153	0.9107	NA	NA	NA	NA	NA	NA	NA	NA	NA	NA	NA	NA
Normalized Error E																		
$\bar{E}$	0.0147						0.0077						0.0205					
σ_E	0.0015						0.0011						0.0004					
$\hat{C}_E$	10.2040						14.2857						1.9512					

Table 4: The mean, the standard deviation and the coefficient of variation estimate by AMBA of the modes of interest of the signals of Towers W, V and X for both the frequency and the damping ratio. The reference values of the estimated frequency modes are found in Tab. 2

	Tower Mont-Blanc						Tower Belledonne						Tower Arpej II					
Region of interest	$8 \leq N_{rds} \leq 10$						$8 \leq N_{rds} \leq 10$						$9 \leq N_{rds} \leq 11$					
mode	$\bar{f}$	σ_f	$\hat{C}_f$	$\bar{\xi}$	σ_ξ	$\hat{C}_\xi$	$\bar{f}$	σ_f	$\hat{C}_f$	$\bar{\xi}$	σ_ξ	$\hat{C}_\xi$	$\bar{f}$	σ_f	$\hat{C}_f$	$\bar{\xi}$	σ_ξ	$\hat{C}_\xi$
1	0.83	0.00006	0.0072	0.57	0.0300	5.2631	0.87	0.0058	0.6666	1.03	0.0900	8.4905	1.27	0.0058	0.4566	1.06	0.0473	4.4622
2	1.07	0.1002	9.3644	0.69	0.0635	9.2028	1.23	0.0577	4.6910	1.14	0.3259	28.5877	5.02	0.0063	0.1254	2.65	0.0451	1.7018
3	3.20	0.0100	0.3125	1.49	0.0153	1.0268	3.03	0.0115	0.3795	0.52	0.3676	69.3584	NA	NA	NA	NA	NA	NA
4	NA	NA	NA	NA	NA	NA	3.27	0.0005	0.0152	1.16	0.0643	5.5431	NA	NA	NA	NA	NA	NA
Normalized Error E																		
$\bar{E}$	0.0110						0.0309						0.0373					
σ_E	0.0004						0.0005						0.0005					
$\hat{C}_E$	3.6363						1.6181						1.3404					

Table 5: The mean, the standard deviation and the coefficient of variation estimate by AMBA of the modes of interest of the signals of Towers Mont-Blanc, Belledonne and Arpej II for both the frequency and the damping ratio. The reference values of the estimated frequency modes are found in Tab. 3

As the damping ratios of the higher modes of the signals in this paper has not been published, hence the need to do the job in this paper with the AMBA method that looks correct when you look at the fundamental mode.

As for tower W and based on the *a priori* information about the signal from [4] (*c.f.*, Tab. 2), it can be seen on Fig. (4 (a)) that AMBA is able to estimate the seven modes of interest starting from N_{rds} equal to 8 periods. These modes are located at around 0.7 Hz, 1.13 Hz, 2.38 Hz, 3.48 Hz, 4.50 Hz, 6.41 Hz, and 6.88 Hz, which are in a well match with the modes estimated by [4] as shown in Fig. (5 (a)). It is worth mentioning here that the seventh mode at around 6.88 Hz was not treated in [4] but it was clearly detected by Fourier Transform, the method they used to estimate the modal frequencies of the signal of tower W (the interested reader could refer to [4] for more clarifications).

Accordingly, N_{rds} greater than or equal to 8 is regarded as the number of periods of the MRDS that is needed to estimate the number of modes in the signal of tower W. The stability of the damping ratio is considered as a criterion to select the most suitable period to estimate the frequencies and the damping ratios of all these modes.

Fig. (4 (b)) shows the estimated damping ratios of all the seven detected modes for N_{rds} between 8 and 12. As could be seen on the figure, the range of N_{rds} between 8 and 12 is split into two regions based on the stability of the estimated damping ratio, 1) $8 \leq N_{rds} \leq 10$, and 2) $10 \leq N_{rds} \leq 12$. At this stage, the stability of the normalized error E (Eq. 5) is considered as a criterion to choose the region with the most reliable modal estimate, and to set the required number of periods in the MRDS.

In Fig. (4 (c)), the normalized error E (Eq. 5) of these two regions is calculated, the first region, $8 \leq N_{rds} \leq 10$, shows a lower standard deviation ($\sigma_E = 0.0015$) which indicates more stability for the estimated damping ratios and natural frequencies. Even though, the damping ratios of the 2^{nd}, 4^{th} and 6^{th} modes are not as stable as the other three modes, and sometimes they show lower values as compared to their previous modes as can be seen in Tab. 4. However, this is attributed to the fact that these modes are from the torsion direction

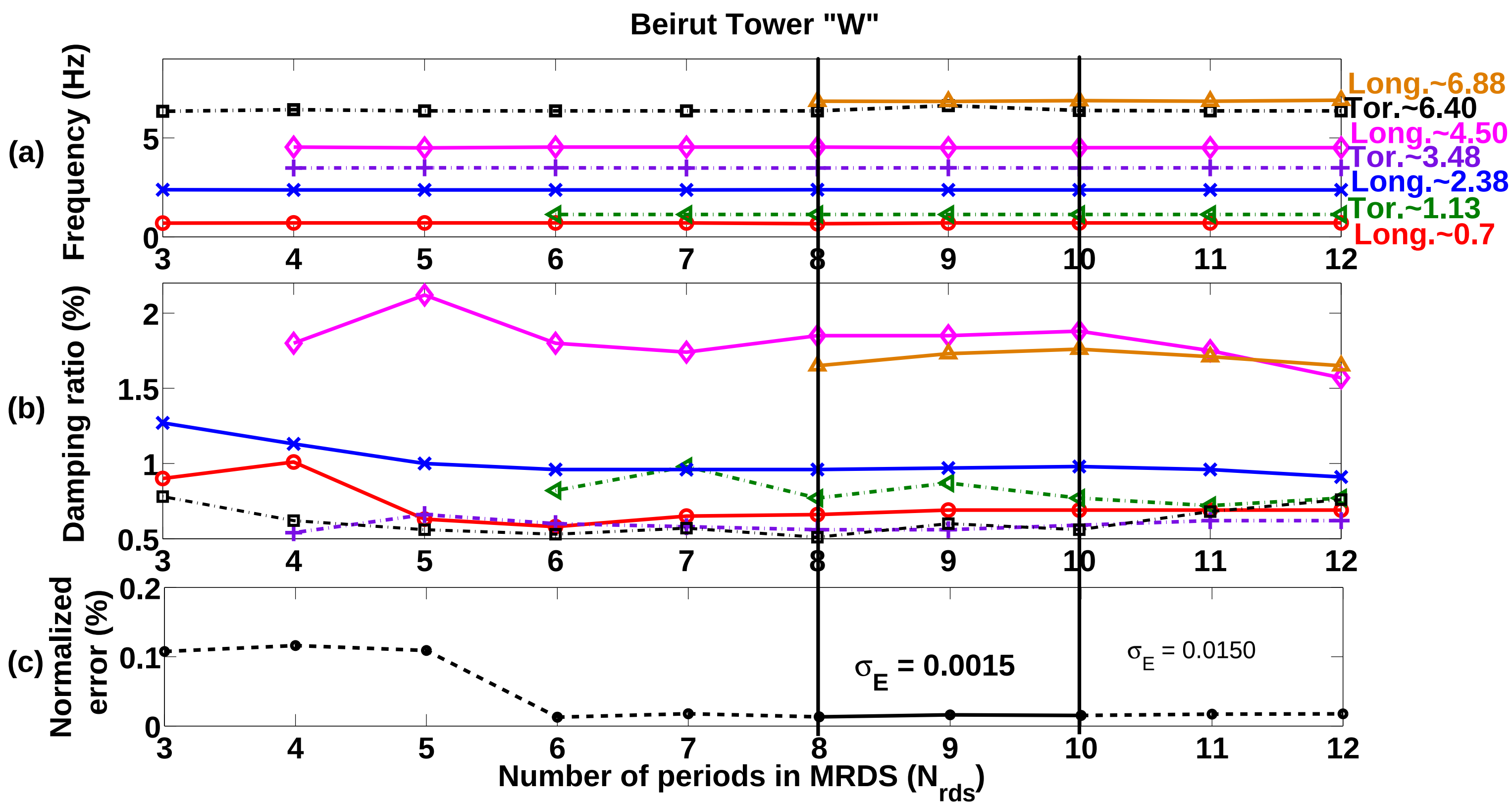

Figure 4: (a) The frequency, (b) the damping ratio and (c) the normalized error estimated by AMBA for tower W in Beirut (Lebanon) in the longitudinal (long.) direction. Tor. indicates the torsion modes observed in the long. direction. σ_E is the standard deviation of the normalized error. The region of interest is indicated by bold σ_E.

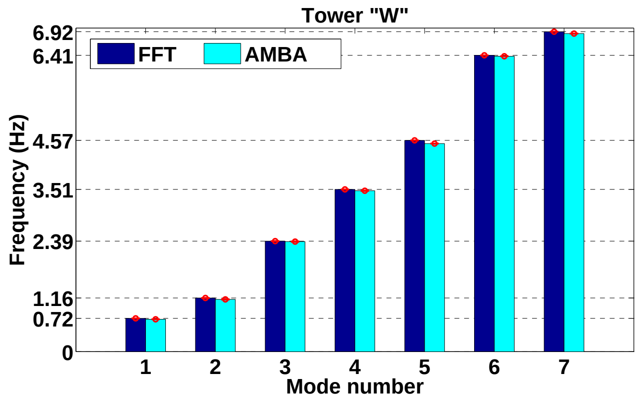

(a)

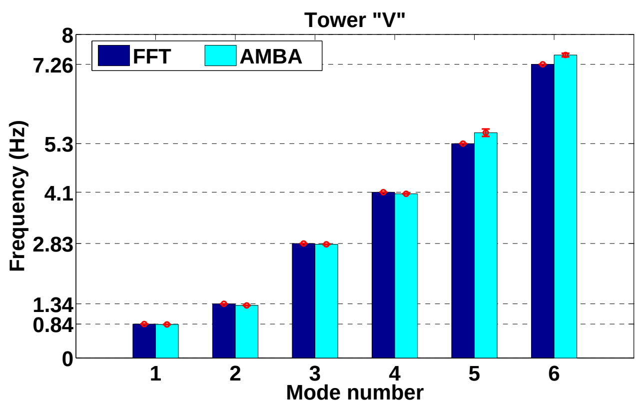

(b)

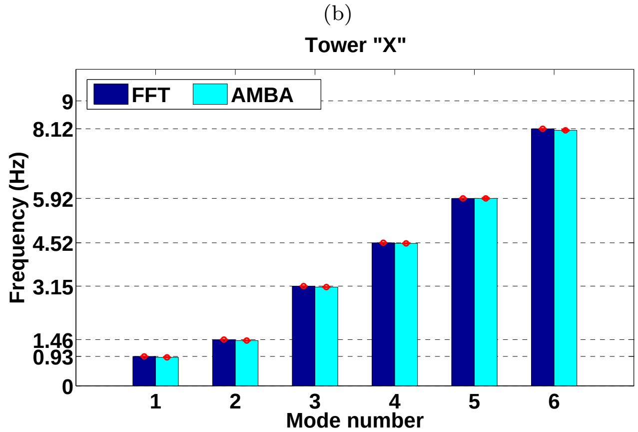

(c)

Figure 5: Mean frequency estimates for the different N_{rds} in the region of interest (light blue), and their associated values that were estimated in [4] by using the Fast Fourier Transform (FFT) (dark blue), along with their standard deviations using AMBA for (a) Tower W, (b) Tower X, and (c) Tower V.

that were only observed in the longitudinal direction. This observation is true for all the other buildings. Generally, the estimation of the modal parameters is less reliable when different directions are considered.

It should be noted that the three towers, W, V and X are very closely located as already mentioned in section 5, and can be seen as sharing the same geological and environmental conditions. They are of the same exact structure, shape and design except that their number of floors is different. In this regard and in the context of our work, we consider that the difference of signal-to-noise ratio (SNR) is only introduced by the difference in the number of floors.

Accordingly, the slightly higher fundamental frequency of tower X as shown in Tab. 4 and Fig. (6) is explained by the shortest height of this tower as it has the least number of stories among the other two towers. Under the very specific background in the context of our work, the signal-to-noise ratio of this tower, is on the other hand, the lowest, as it increases with the number of stories, thus it is the tower that is more sensitive to noise.

Tower V (Fig. 7), on the other hand, experiences a medial values for both the fundamental frequency and the normalized error E among towers W and X. This is also explained by its medial number of stories.

Consequently, the ascending order of the mean normalized error $\bar{E}$ of the three towers W, V and X as shown in Tab. 4 with respect to their number of stories could thus justify the counter relationship between the SNR and the number of stories of the building.

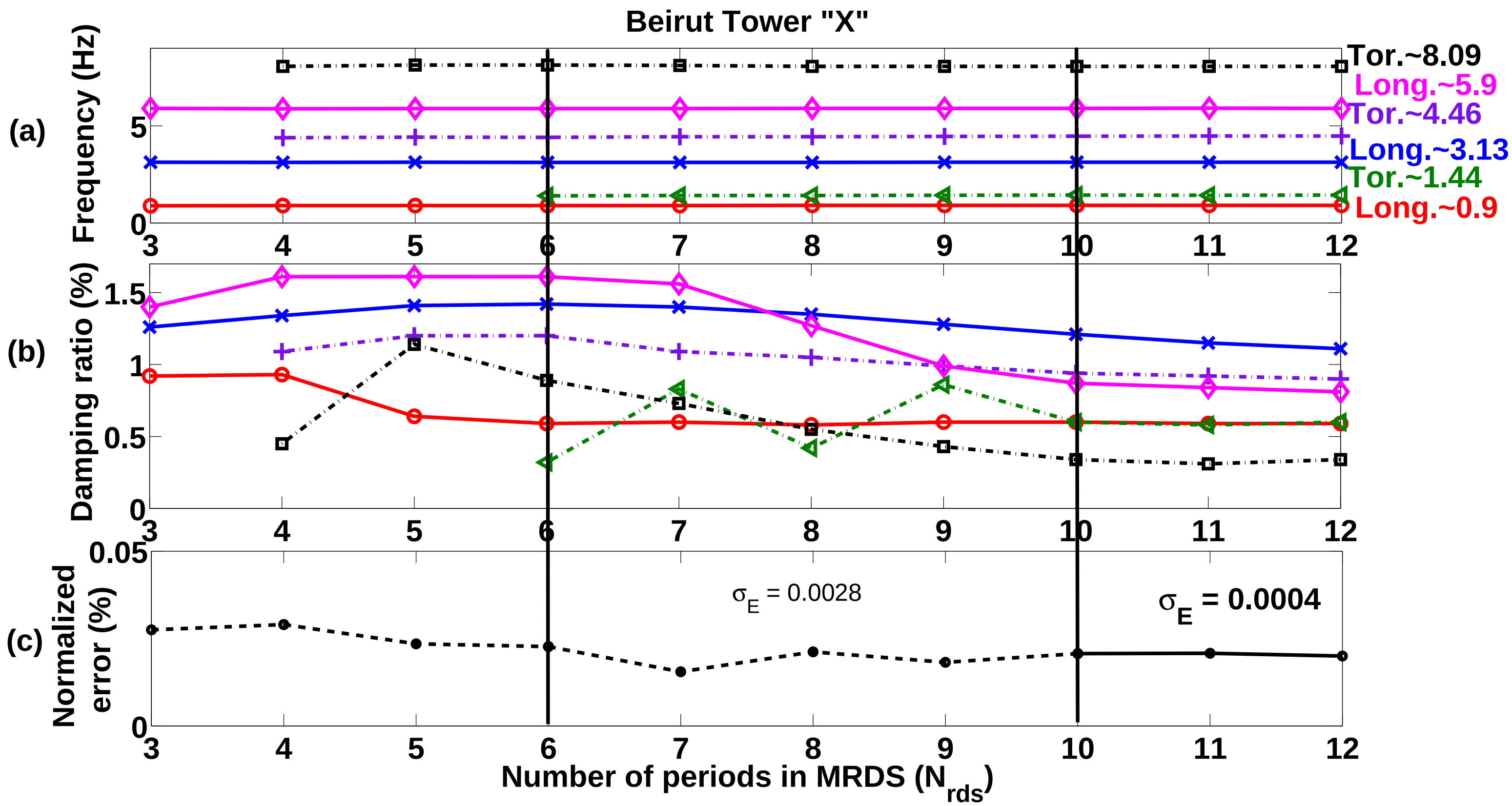

Figure 6: (a) The frequency, (b) the damping ratio and (c) the normalized error estimated by AMBA for tower X in Beirut (Lebanon) in the longitudinal (long.) direction. Tor. indicates the torsion modes observed in the long. direction. σ_E is the standard deviation of the normalized error. The region of interest is indicated by bold σ_E.

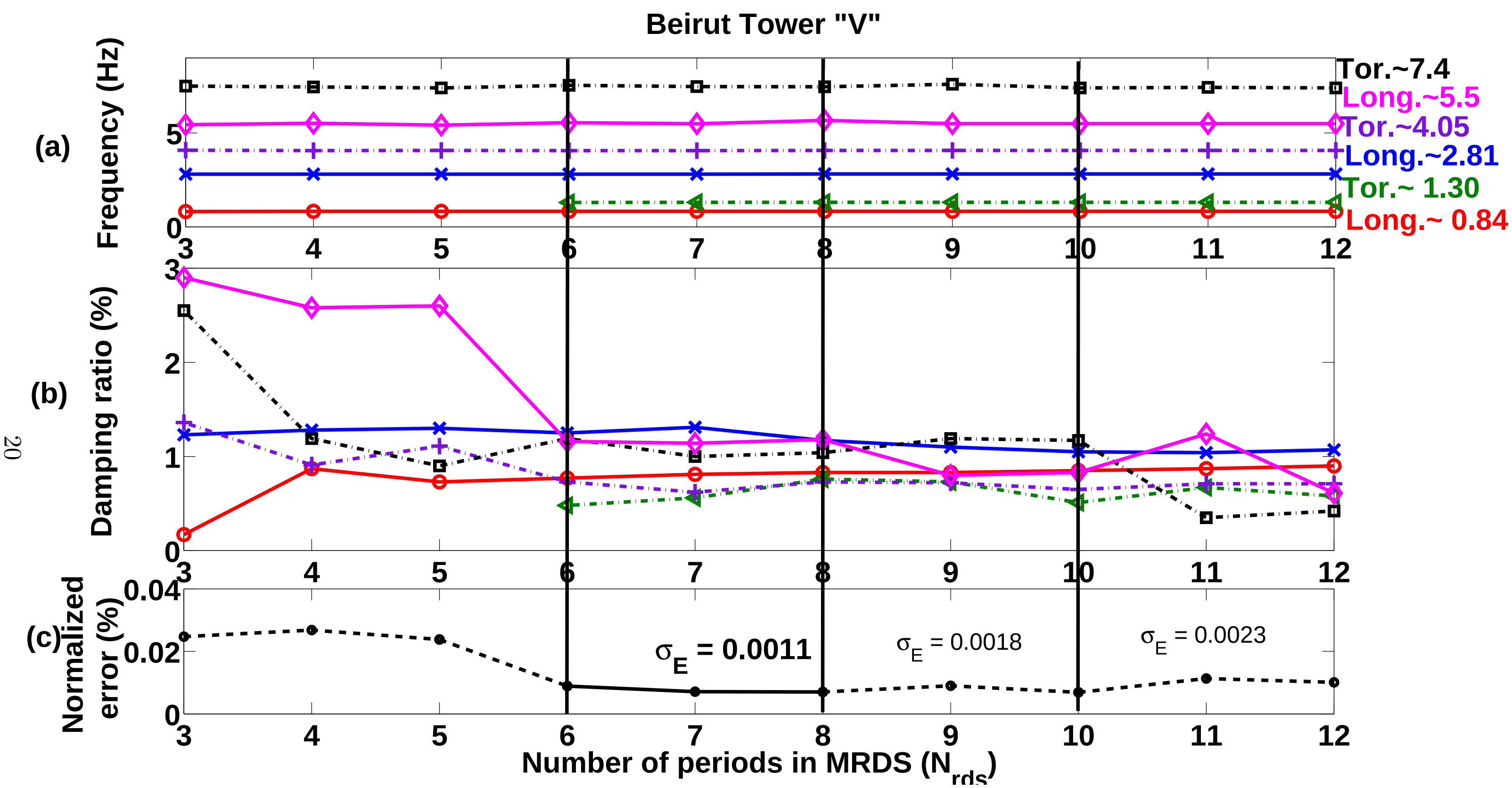

Figure 7: (a) The frequency, (b) the damping ratio and (c) the normalized error estimated by AMBA for tower V in Beirut (Lebanon) in the longitudinal (long.) direction. Tor. indicates the torsion modes observed in the long. direction. σ_E is the standard deviation of the normalized error. The region of interest is indicated by bold σ_E.

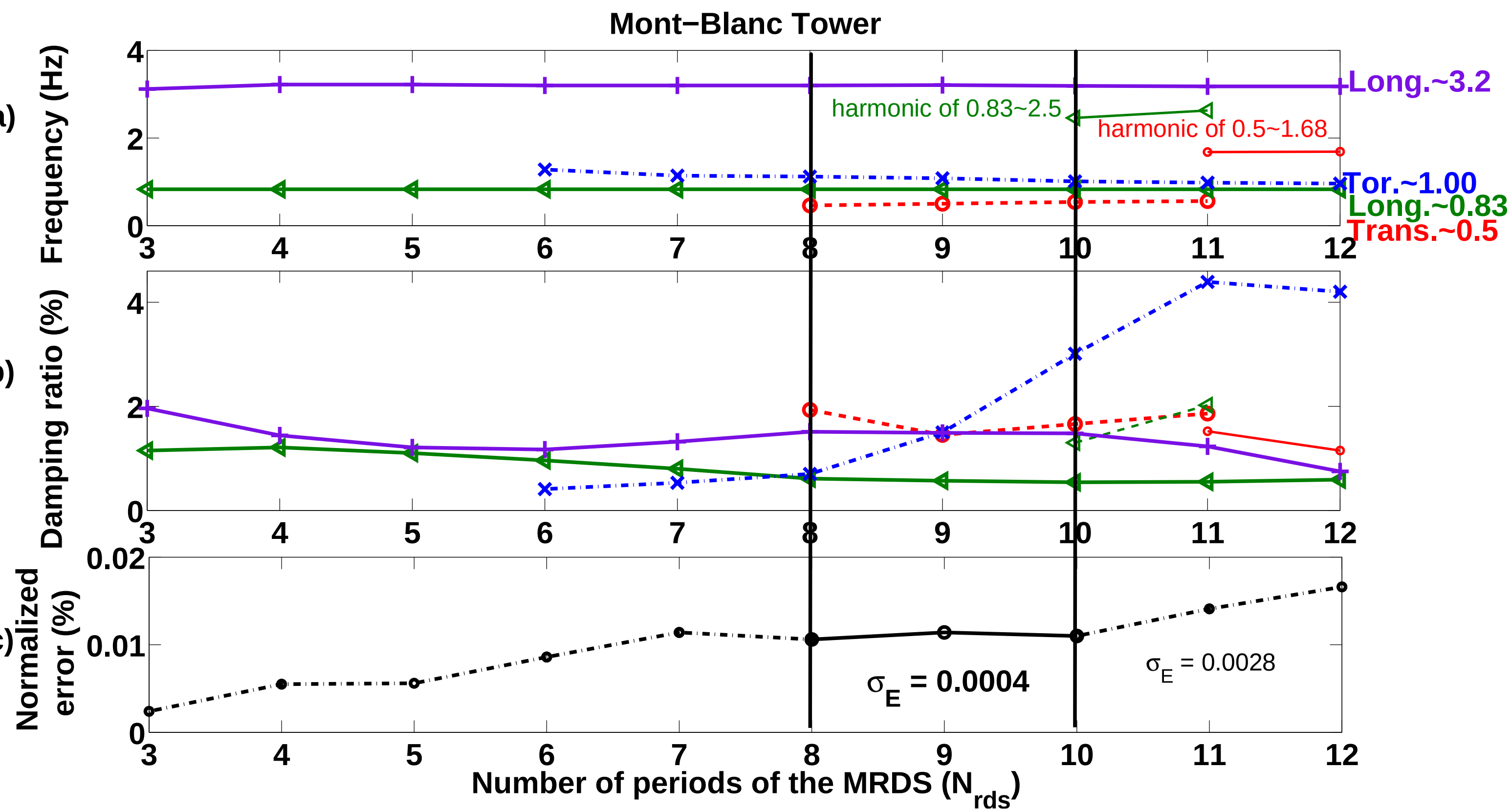

Figure 8: (a) The frequency, (b) the damping ratio and (c) the normalized error estimated by AMBA for tower Mont-Blanc in Grenoble (France) in the longitudinal (long.) direction. Tor. and Trans. indicates respectively the torsion and the transverse modes observed in the long. direction. σ_E is the standard deviation of the normalized error. The region of interest is indicated by bold σ_E.

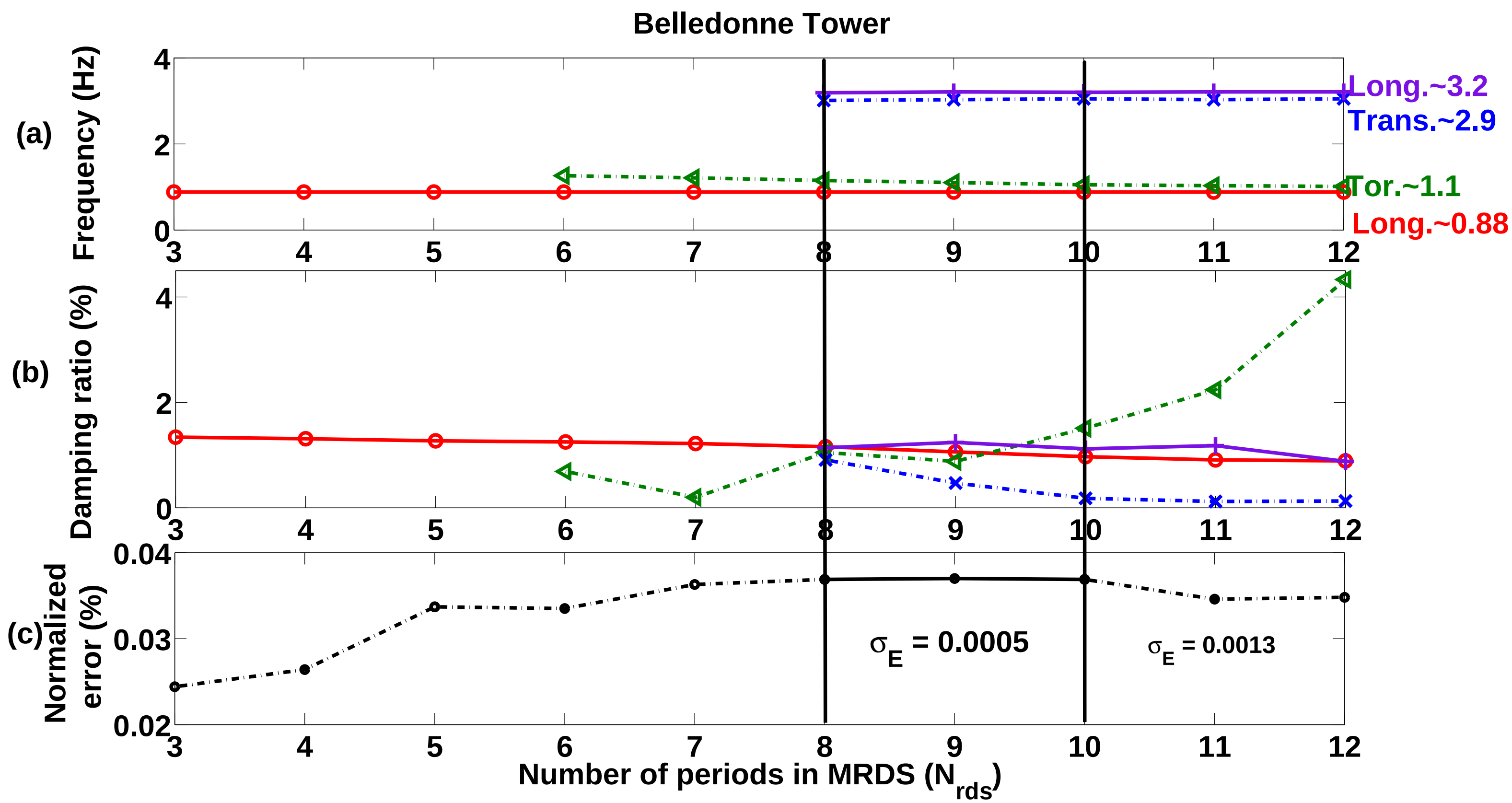

Figure 9: (a) The frequency, (b) the damping ratio and (c) the normalized error estimated by AMBA for tower Belledonne in Grenoble (France) in the longitudinal (long.) direction. Tor. and Trans. indicates respectively the torsion and the transverse modes observed in the long. direction. σ_E is the standard deviation of the normalized error. The region of interest is indicated by bold σ_E.

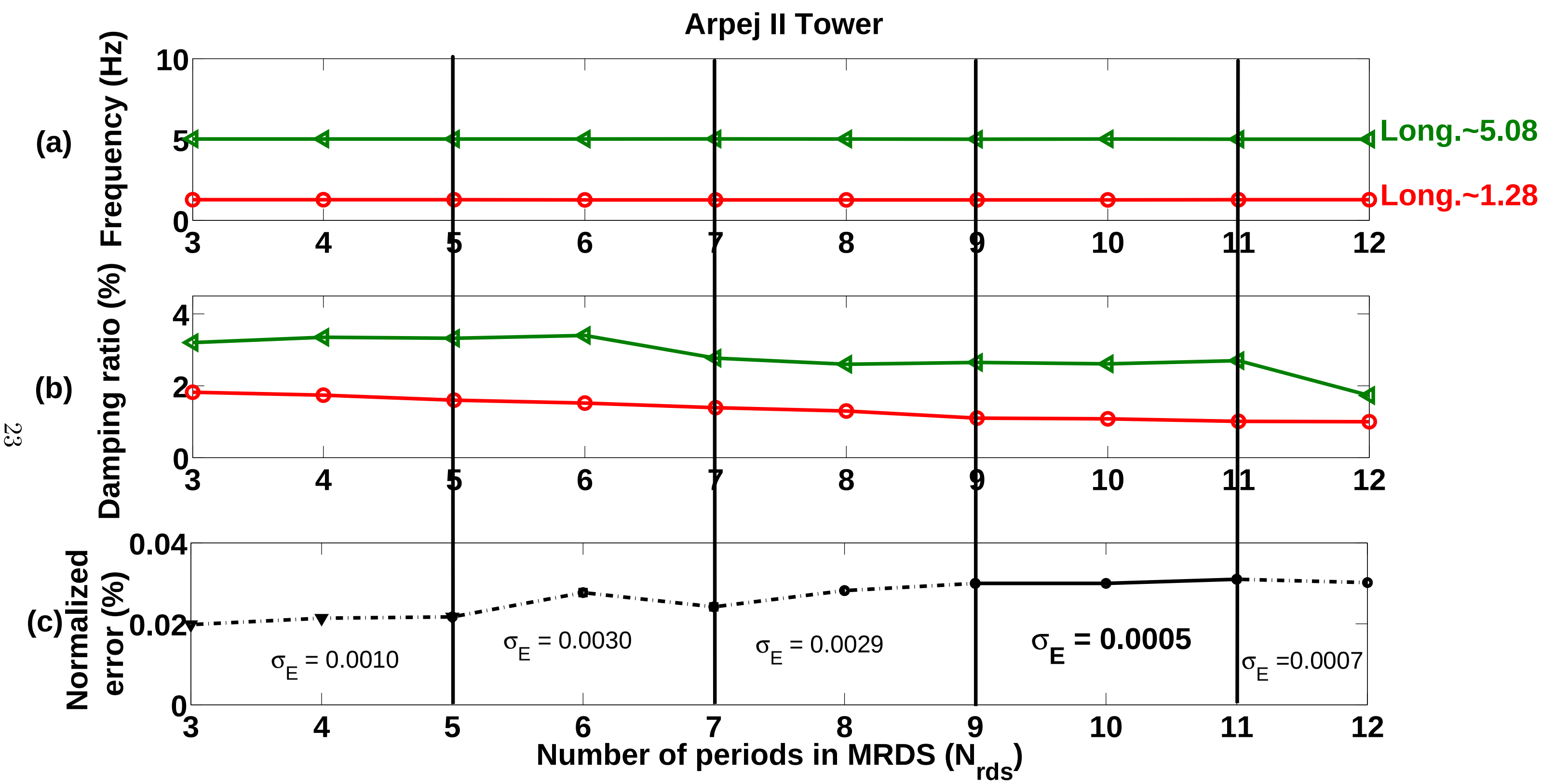

Figure 10: (a) The frequency, (b) the damping ratio and (c) the normalized error estimated by AMBA for tower Arpej II in Grenoble (France) in the longitudinal (long.) direction. σ_E is the standard deviation of the normalized error. The region of interest is indicated by bold σ_E.

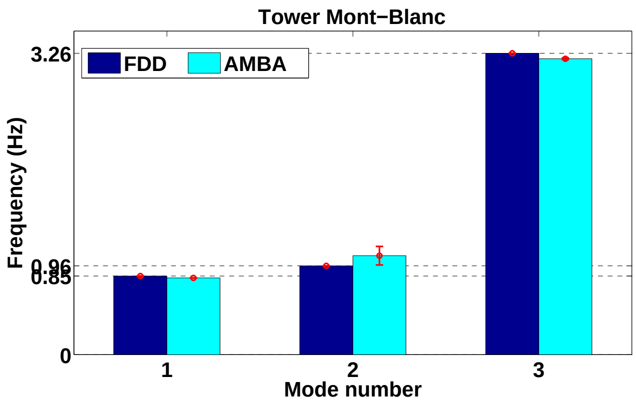

(a)

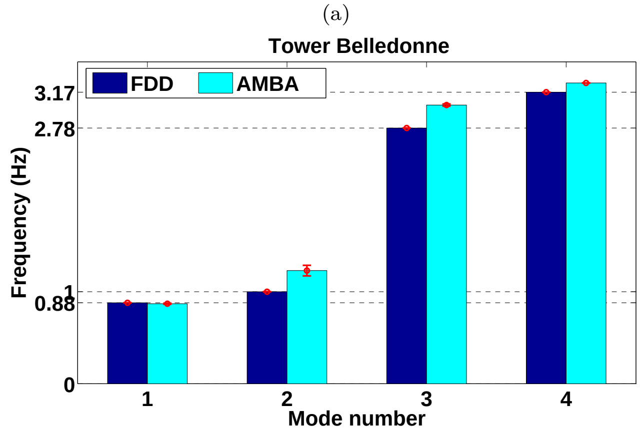

(b)

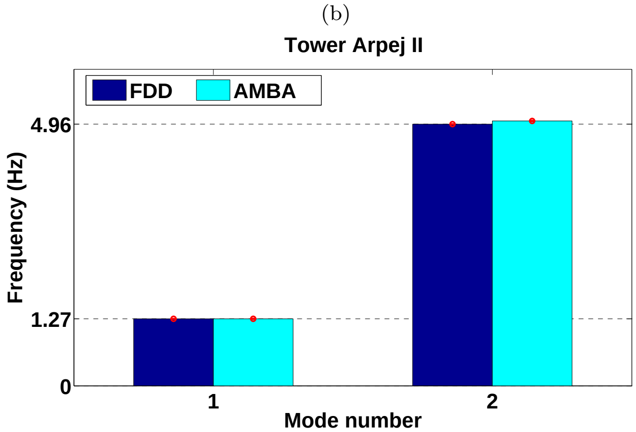

(c)

Figure 11: Mean frequency estimates for the different N_{rds} in the region of interest (light blue), and their associated values in [5, 6] using the Frequency Domain Desomposition (FDD) (dark blue), along with their standard deviations using AMBA for (a) Tower Mont-Blanc, (b) Tower Belledonne, and (c) Tower Arpej II.

The same trend as those of Beirut towers is also observed over these of Grenoble towers, *i.e.*, Arpej II tower is half the height of those of Mont-Blanc and Belledonne, and thus as shown in Tab. 5, its fundamental frequency is higher and its mean normalized error is the highest. A well matching between the results of AMBA and those of [6, 7] is clearly illustrated in Fig. (11) for all the three towers.

In figures (8) and (9) for towers Mont-Blanc and Belledonne respectively, the torsion mode is clearly visible at around 1 Hz. The standard deviation of the torsion mode for both towers is higher than that of the other modes, this can be attributed to the fact that this mode is not in the direction of study of these two signals, *i.e.*, the longitudinal direction. Another mode at around 3 Hz is detected for tower Belledonne, this is the transverse mode that is observed in the longitudinal direction of this building which also explains its unstable damping ratio estimates.

For the frequency estimate, AMBA has shown a very well match with the results of [4, 5, 6, 7]. Moreover, AMBA was able to do the estimation of all the modes of the signal simultaneously and automatically. More and above, reliable estimates of the damping ratio were also provided by AMBA, the results of the latter were only disturbed when the estimated mode is not in the chosen direction of study.

7. Conclusions

This paper handled the application of an already proposed Automatic Model-Based Approach (AMBA) [1] for the automatic estimation of the frequency and the damping ratio of multi-component real-world signals.

As per [1], AMBA proved itself to be applicable over a single-channel record, not to be restricted to SDOF systems, i.e., having the ability to deal with multi-mode ambient vibration signals, and to take into consideration the estimation of the damping ratio, and the closely-spaced frequency modes. It is also capable of distinguishing the true modes from the noisy ones thanks to an automatic peak-detection method which avoids any user interaction.

In this paper, six actual high-rise buildings subjected to real-world ambient vibrations were chosen to validate AMBA. Three of them (Towers W, X and V) are in Beirut (Lebanon), and the other three (Mont-Blanc, Belledonne, and Arpej II) are in Grenoble (France). These buildings are chosen due to their interesting characteristics. The three towers of Beirut follow the same construction design and are settled in the same geological formation, they assumed to only differ in the number of stories. Mont-Blanc and Belledonne, on the other hand, are considered similar in terms of design, shape and height. Arpej II has half the height of the latter two towers.

The main challenge to the estimator when dealing with real-world ambient vibrations is that no *a priori* knowledge of the number of modes, neither the modal frequencies nor the damping ratio is available. AMBA was applied to deal with such a situation by first an initialization step, which requires no *a priori* information and provides a rough modal estimates; and second a Maximum-Likelihood Estimation step, which refines the estimates of the initialization step and provides final non-biased modal estimates.

However, the initialization step of AMBA is spectral-based. Thus the estimated number of modes is related to the frequency resolution of the used spectrum. To solve this issue, and in order to deal with multi-component signals which is always the case of the real-world ambient vibration signals, we proposed in this paper a method to automatically choose the best segment length N_{rds} in the Random Decrement Technique that constitute the basis of AMBA.

The algorithm defines automatically the best N_{rds} as the one that is capable of detecting the highest number of modes with the most stable damping ratio and normalized error between the estimated and the reconstructed Multi-mode Random Decrement Signature. Based on these criteria, the best N_{rds} is then provided to the next step of AMBA to simultaneously and automatically estimate the natural frequencies and the damping ratios of all the modes of the signal under study.

The highest buildings are expected to have lower fundamental frequencies and higher signal-to-noise ratio, and they are known to be less sensitive to noise. AMBA was able to demonstrate this phenomena over the six studied buildings. The estimated fundamental frequency of tower X (16 stories) is the highest with the highest mean normalized error as compared to towers V (18 stories) and W (21 stories). Similarly for tower Arpej II (16 stories) as compared to Mont-Blanc and Belledonne (30 stories).

However, as Mont-Blanc and Belledonne are identically designed, they could present the same modal estimates. These buildings can differ in their foundations, the quality of the used materials, the occupancy, the environmental conditions and so on, which affects their dynamic characteristics. Nevertheless, close modal estimates should be obtained. Such results were clearly illustrated by AMBA as the two towers presented slightly different estimated modal results.

All the obtained results by AMBA were cross validated with several references analyzing the same buildings with a manual modal analysis [4, 5, 6, 7]. AMBA matches well with these results but in a simultaneous and automatic way. Moreover, it is able to provide a reliable estimation for the damping ratios.

In the future, in order to improve the estimation quality of AMBA, the estimation of the number of modes should be integrated in a parametric model. Moreover, AMBA should be tested in the analysis of long-term frequency and damping time-tracking in high-rise buildings. Even though, it is not possible to assess the mode shapes using only one single sensor, and this was not the main goal of the manuscript but effectively it could be imagined to deal with this point in the future as well.

Acknowledgements

This work has been supported by French Research National Agency (ANR) through RISKNAT program (project URBASIS ANR-09-RISK-009) to get the data collected in Granoble (France), and by the LIBRIS ANR (ANR-09-RISK-006) project by Armand Mariscal and Christophe Voisin (ISTerre) to get the data collected in Beirut (Lebanon).

References

[1] F. Nasser, Z. Li, N. Martin, P. Gueguen, An automatic approach towards modal parameter estimation for high-rise buildings of multicomponent signals under ambient excitations via filter-free random decrement technique, Journal of Mechanical Systems and Signal Processing (Sep. 2015).

[2] C. Boutin, S. Hans, E. Ibraim, P. Roussillon, In situ experiments and seismic analysis of existing buildings. part ii: Seismic integrity threshold, Earthquake engineering & structural dynamics 34 (12) (2005) 1531–1546.

[3] M. Perrault, P. Gueguen, A. Aldea, D. Sorin, et al., Reducing the uncertainties of the fragility curves using experimental testing in existing buildings: the case of the brd tower of buccarest (romania), Earthquake Engineering and Engineering Vibration (2013) 12 (4).

[4] P. Gueguen, C. Voisin, A. Mariscal, Wandering of the modal parameters in existing building: application to structural health monitoring and seismic vulnerability analysis., Proceedings of The 15th WCEE, LISBOA (2012).

[5] A. Mikael, P. Gueguen, P.-Y. Bard, P. Roux, M. Langlais, The analysis of long-term frequency and damping wandering in buildings using the random decrement technique, Bulletin of the Seismological Society of America 103 (1) (2013) 236–246.

[6] C. Michel, P. Gueguen, M. Causse, Seismic vulnerability assessment to slight damage based on experimental modal parameters, Earthquake Engineering & Structural Dynamics 41 (1) (2012) 81–98.

[7] M. Valla, P. Gueguen, B. Augere, D. Goular, M. Perrault, Remote modal study of reinforced concrete buildings using a multipath lidar vibrometer, ASCE Journal of Structural Engineering (2015) 141 (1).

[8] P. Guéguen, M. Valla, B. Augère, D. Goular, et al., Analysis of reinforced concrete buildings using multipath lidar, in: EWSHM-7th European Workshop on Structural Health Monitoring, (2014).

[9] P. Gueguen, Seismic vulnerability of structures, John Wiley & Sons, (2013).

[10] H. A. Cole, On-the-line analysis of random vibrations, AIAA Paper (1968) 68–288.

[11] S. Kirkpatrick, Optimization by simulated annealing: Quantitative studies, Journal of statistical physics 34 (5-6) (1984) 975–986.